Five-bit substrate guided wave true-time delay module working up to 2.4 THz with a packing density of 2.5 lines/cm^2 for phased array antenna applications

Zhenhai Fu, MEMBER SPIE
Ray T. Chen, MEMBER SPIE
University of Texas at Austin
Microelectronics Research Center
Department of Electrical and Computer Engineering
Austin, Texas 78758
E-mail: raychen@uts.cc.utexas.edu

Abstract. A 5-bit true-time delay module is demonstrated. The combination of a 1-to-4 fiber beamsplitter and four 1-to-8 collinear guided-wave fanouts provides us with the required 32 surface-normal fanout beams with a delay step of 50 ps. The system design, device fabrication, and optimization of the fanout intensity uniformity down to ±10% among 32 fanouts are addressed. The packing density of this device is 2.5 (delay lines)/cm^2, which is the highest demonstrated thus far. A bandwidth of 2.4 THz is confirmed experimentally by employing a femtosecond laser and an ultrafast detector. [S0091-3286(98)03006-2]

Subject terms: phased array antennas; true-time delay.

Paper 47077 received July 25, 1997; revised manuscript received Oct. 30, 1997, and Feb. 14, 1998; accepted for publication Feb. 17, 1998.

1 Introduction

Phased array antenna (PAA) systems combine the signals from multiple stationary antenna elements with the same frequency to point a directive beam at a certain angle in space. The characteristics and angles of the beams are selected across the array elements by controlling the amplitude and/or the phase of encoded carriers.[1] In order to satisfy the ultrawide bandwidth requirements of phased array antennas, it is necessary to implement true-time delay (TTD) steering techniques. In the TTD approach, the microwave phase shift at each antenna element, which is proportional to the microwave frequency, can follow the frequency change without creating a drift of the beam steering angle. Therefore, the far-field pattern is independent of the frequency employed.[2]

For real system implementations of TTD beam steering, a specific beam-forming direction is achieved by selecting a true-time delay setting. In order to scan the beam into another angle, a completely different configuration of the delays has to be established. Thus, it is usually impractical to realize continuously tuned TTD with a large steering angle. Most existing TTD beam-steering systems adopt the following two approaches. First, the array elements are grouped into M subarrays, each with its own common time delay. The bandwidth of an array of M subarrays is M times that of the phase-steering array.[3] Second, each time-delay unit is built to provide a discrete set of delay lines. The set of discrete time-delay increments selected for each steering angle represents a ''quantized'' approximation to a linear phase taper. In general, a higher degree of accuracy requires a smaller time-delay increment and more bits of resolution. In this way, the system provides some, but not all, of the benefits of true-time delay steering. Compared with electrical TTDs, photonic TTDs offer wider bandwidth, compact size, reduced weight, low high-frequency rf loss, and lower electromagnetic interference (EMI).[4] Various types of photonic TTD delay units have been demonstrated by a few research groups, such as fiber delay lines,[5,6] fiber optic Bragg grating TTD elements,[7] waveguide optical time-shift networks,[8–10] acousto-optic TTD elements,[11] and multiwavelength WDM TTD lines.[12] These TTD lines do have some advantages, such as accurate time delay and monolithic integration with detectors, but they suffer from some disadvantages, such as the many light sources, switches, and modulators needed, low packing density, complexity in fabrication and control, and high loss.

In this paper, a 5-bit (2^5) true-time delay unit with a packing density of 2.5 lines/cm^2, distributing broadband microwave signals having a delay step of 50 ps for phased array antennas, is accomplished through the combination of a 1-to-4 fiber beamsplitter and four 1-to-8 substrate guided wave optical fanouts. Substrate guided waves are used as carriers for distributing and delaying the microwave signals driving the antenna radiating elements. The design and fabrication of the planar holographic gratings are discussed. Fanout power fluctuation is discussed next. A delay interval of 50 ps and bandwidth measurement up to 2.4 THz are demonstrated.

2 System Design

Figure 1 shows the basic system architecture of our 5-bit device.[13,14] The 2-D substrate guided wave optical elements are used for successive optical delays of up to 32 $\Delta\tau$. A 1-to-4 fiber beamsplitter with predetermined fiber lengths is used to provide four delay signals, each with eight $\Delta\tau$ delay increments. Each of the delay signal from the 1-to-4 beamsplitter is coupled into the substrate surface-

 0091-3286/98/$10.00

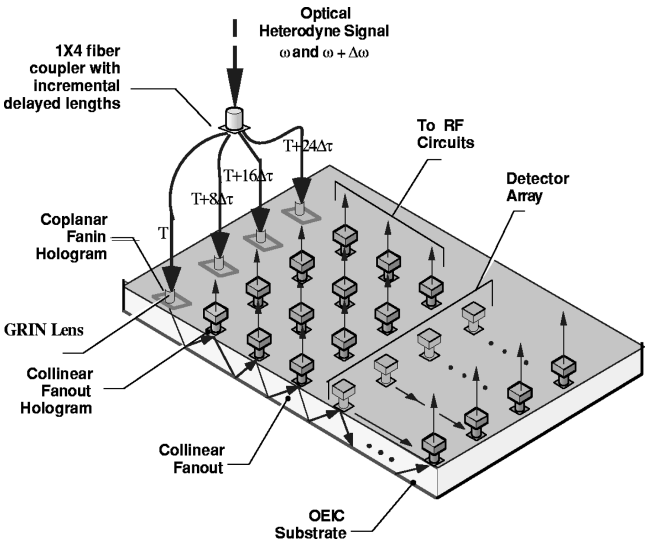

Fig. 1 Five-bit optical delay lines based on substrate guide mode with holographic grating couplers.

normally with a specific substrate bouncing angle through a holographic coupler and then zig-zags within the substrate through total internal reflection (TIR).[15,16] Portions of the substrate guided waves are sequentially extracted surface-normally through a holographic output coupler array as shown in Fig. 2. Different optical delays are obtained at subsequent fanouts within the substrate. The time delay between two successive collinear fanouts is $\Delta\tau$. Thus, 32 (2^5) delay lines are achieved. The fanout optical signals are detected by a two-dimensional high-speed photodetector array and then sent to antenna transmitters by programmed electronic switching devices. The TTD architecture reported herein offers compactness and the required wide instantaneous bandwidth. It is feasible to achieve TTD devices with different delay steps and more bits of delay lines based on this architecture. The potential advantage of integrating a 2-D detector array surface-normally is to eliminate the delicate interface between the optical delay lines and the rf switching circuits. Due to the collinear multiplexibility of the delay lines, a high packing density can be achieved. On the other hand, the device does have a major disadvantage, which is the 1-to-32 fanout loss. However, with the use of an erbium-doped fiber amplifier (EDFA) and a working wavelength of 1550 nm, this loss can be compensated.

The true-time delay unit reported herein can be used not only to provide true-time delay signals to one antenna element, but also to provide delay signals to several antenna elements simultaneously. In the case of one 5-bit TTD unit controlling one antenna element, an example is shown in Fig. 3(a), where the PAA is programmed to steer from $-\Phi$ to $+\Phi$. Numerically, $\Phi=45$ deg is chosen as the case of study. For the 5-bit TTD unit, the smallest differential delay increment is given by[13]

$$\Delta\tau=\frac{L\ \sin\theta_{\max}}{31c}, \tag{1}$$

where L is the linear dimension of the linear PAA. Assume $L=65$ cm; then $\Delta\tau=50$ ps. Here, only one detector's output, which has the desired delay, is connected to the antenna element at one time to stare in one direction while all the other detectors are disconnected. To stare into another direction, another detector's output with another desired delay is connected to the antenna element. In this approach, the device suffers from a high loss because only one of the 32 delay signals is used at one time.

For the case of one 5-bit TTD unit controlling multiple antenna elements, an example is shown in Fig. 3(b), where a 5-bit module is used as four 3-bit units to control five antenna subarrays (one of these five subarrays is provided with zero-delay signal). Each subarray has four antenna elements, which share the same delay signals. A phase shifter is behind each antenna element to fine-tune the phase delay and thereby scan with a small angle increment. Similarly, suppose the PAA is programmed to steer from $+45$ to -45 deg, and $L=85$ cm. The possible scanning angles and the corresponding delay signals needed by each subarray are shown in Table 1, where $\Delta\tau$ is set at 50 ps. As shown in Fig. 3(b) and Table 1, to stare in one direction, say -45 deg, the microwave switches behind the subarrays connect the desired delay signals of 0, 8 $\Delta\tau$, 16 $\Delta\tau$, 24 $\Delta\tau$, and 32 $\Delta\tau$ to subarrays 1, 2, 3, 4, and 5, respectively. To stare into another direction, say $+32$ deg, the switches controlled by the control signals send delay signals of 24 $\Delta\tau$, 18 $\Delta\tau$, 12 $\Delta\tau$, 6 $\Delta\tau$, and 0 to the corresponding subarrays. In such an arrangement, the antenna array can be easily controlled by one 5-bit true-time delay module and an electronic switch chip instead of five different 3-bit TTD modules with different delay steps. Similarly, a 6-bit TTD module based on the structure described in this paper can serve as eight 3-bit units or four 4-bit units, a 7-bit module can serve as sixteen 3-bit units or eight 4-bit units or four 5-bit units, and so on. Therefore, the signal loss is much less, and the weight and cost of the system are dramatically reduced.

To demonstrate a TTD unit shown in Fig. 1 with a delay step of 50 ps, a precise design of the substrate total internal bounding angle θ (as shown in Fig. 2) is needed. With a total internal bouncing angle of θ, the optical delay between successive output couplers is given by

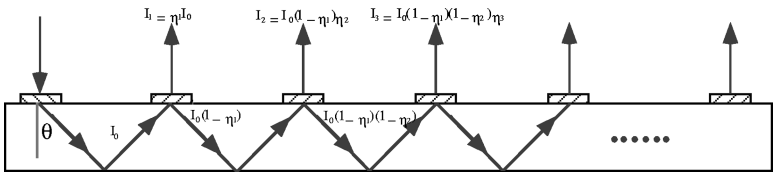

Fig. 2 Optical delay lines based on substrate guided mode together with holographic grating couplers.

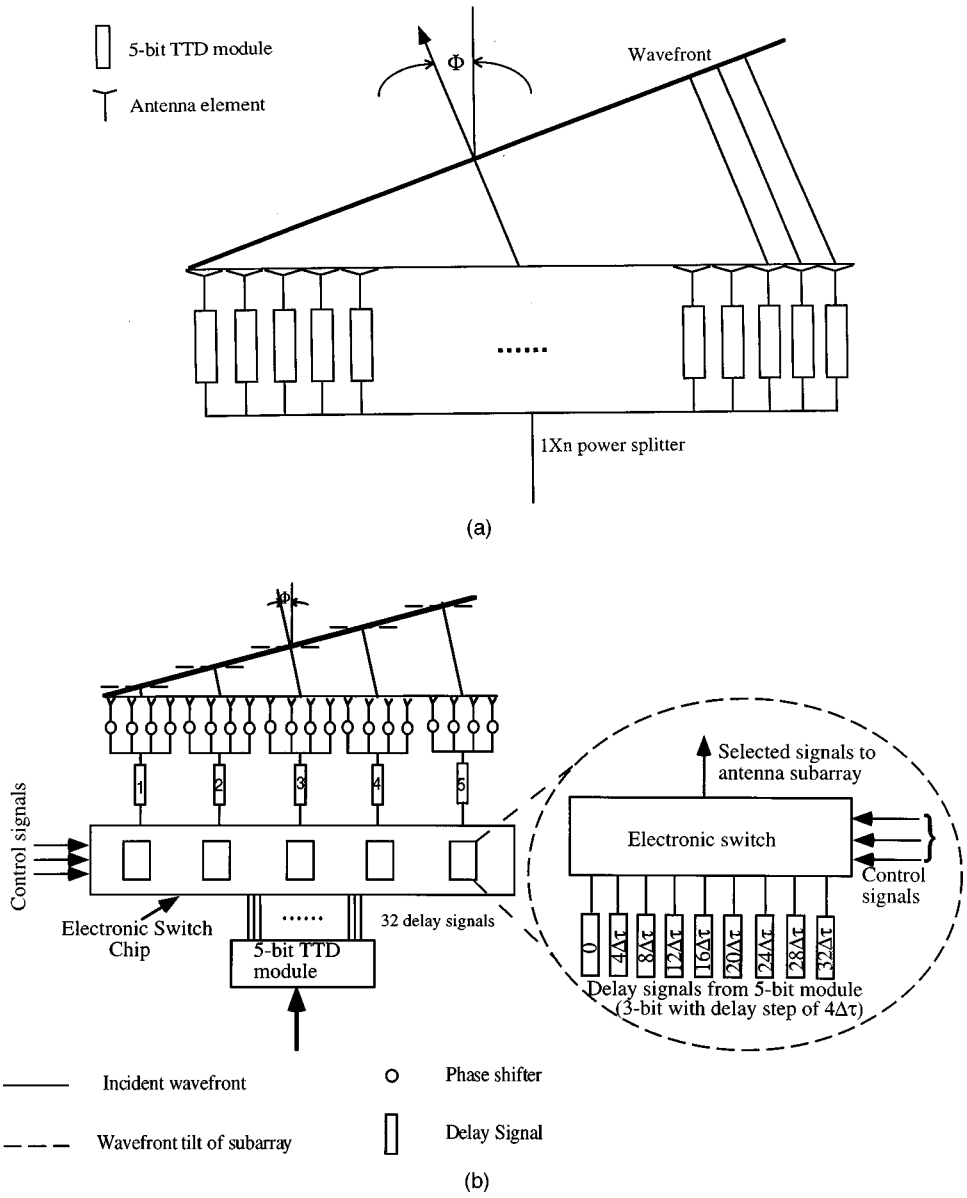

Fig. 3 Wideband scanning array feeds: (a) each unit controls one antenna element; (b) each unit controls five subarrays.

$$\Delta\tau = \frac{\Delta L'}{c/n} = \frac{2d/\cos\,\theta}{c/n} \tag{2}$$

where $\Delta L'$ is the difference of propagation length between two successive fanouts, d is the substrate thickness, c is the speed of light, and n is the refractive index of the substrate material.[13] For a 50-ps delay, one possible thickness d of the quartz substrate is 3 mm, the corresponding θ is 53.5 deg, and the distance between two successive fanouts is 8 mm. Figure 2 illustrates a structure for one of the four TTD subunits with delay paths provided by cascaded substrate guided optical fanouts. The input holographic grating coupler is designed to couple the surface-normal incoming light into a substrate guided mode having a fixed bouncing angle of 53.5 deg. The output holographic grating couplers extract an array of substrate guided beams into a free-space one-dimensional (1-D) array having eight surface-normal fanout beams.

3 Device Fabrication

The input and output holographic couplers can be made from silver halide dichromated gelatin (DCG) films or from other photopolymer holographic recording films. Here these gratings are created by holographic recording using DuPont photopolymer films (HRF 600X001), due to their achievable high diffraction efficiencies and amenability to dry processing after exposure. The two-beam interference method is used to define individual holographic gratings, each at a different recording angle, generating a sinusoidal phase modulation profile.[16–19] Here the recording and re-

Table 1 Scanning angles and the corresponding delays of each subarray.

Scanning angle (deg)	Delay (units of $\Delta\tau$)					Scanning angle (deg)	Delay (units of $\Delta\tau$)				
	Subarray 1	2	3	4	5		Subarray 1	2	3	4	5
−45	0	8	16	24	32	45	32	24	16	8	0
−38.2	0	7	14	21	28	38.2	28	21	14	7	0
−32	0	6	12	18	24	32	24	18	12	6	0
−26.2	0	5	10	15	20	26.2	20	15	10	5	0
−20.7	0	4	8	12	16	20.7	16	12	8	4	0
−15.4	0	3	6	9	12	15.4	12	9	6	3	0
−10.2	0	2	4	6	8	10.2	8	6	4	2	0
−5.1	0	1	2	3	4	5.1	4	3	2	1	0
0	0	0	0	0	0	0	0	0	0	0	0
Delay step:	0	1	2	3	4	Delay step:	4	3	2	1	0

constructing parameters are selected so that the Bragg condition is satisfied. Therefore, there is only one diffraction order.

The hologram recording procedure on DuPont HRF-600 film consists of recording, UV cure, and postbaking. HRF 600X001-20 was selected as the recording material because it exhibits a low scattering loss and a high diffraction efficiency. The film is 20 μm thick. The hologram recording mechanism in the photopolymer is known to be a three-step process. First, an initial exposure records the interference pattern, which causes the initial polymerization and diffusion of the monomer molecules to bright fringes. A higher concentration of polymerization means a higher refractive index. Second, uniform UV light is required for dye bleaching and complete polymerization. Third, baking is done to enhance the index modulation. The maximum refractive index modulation in this type of photopolymer film has been reported to be $\sim$0.04,[20] and a large dynamic range of diffraction efficiency as a function of exposure time can also be achieved by adjusting the light intensities of the two recording beams. The 514-nm line from an argon ion laser is employed as the recording wavelength.

One common problem related to massive substrate guided optical fanout is that the fanout light intensity drops along the light propagation direction. This is caused by the cascaded fanouts if the output couplers have more or less the same efficiency. Substrate absorption also contributes to the problem. For a practical device, it is desired that the collinear multiplexed beams with true-time delay paths be uniformly coupled out surface-normally. A uniform light intensity will relax the responsivity requirements for wideband fast detectors, hence achieving a well-balanced signal-to-noise (S/N) ratio at the microwave end.[13] This is critical, since signal integrity at terms of gigahertz is stringently restricted by the S/N ratio requirements and by the limited detector responsivities. To overcome these problems, the coupling efficiencies of the holographic output couplers have to be individually tuned, which is often a challenging task. To ensure a uniform fanout, it is necessary to precisely tune the diffraction efficiency η_k of the kth coupler, $k=1,2,\ldots,N$. In general,

$$\eta_k=\frac{\eta_1}{1-(k-1)\,\eta_1},\quad k=1,2,3,\ldots,N. \tag{3}$$

Depending on the value of N and the maximum diffraction efficiency achievable for each holographic grating, the diffraction efficiency of each element can be determined. In our case, $N=8$, and assuming that $\eta_8=90\%$, the diffraction efficiencies for $k=1,2,\ldots,7$ are determined to be $\eta_1=12.3\%$, $\eta_2=14\%$, $\eta_3=16.3\%$, $\eta_4=19.5\%$, $\eta_5=24.2\%$, $\eta_6=32\%$, $\eta_7=47\%$.

To achieve the desired diffraction efficiencies, we first derive the relationship governing the diffraction efficiency as a function of the exposure dosage as shown in Fig. 4. The holographic output couplers are accordingly recorded with different exposure dosages to achieve desired efficien-

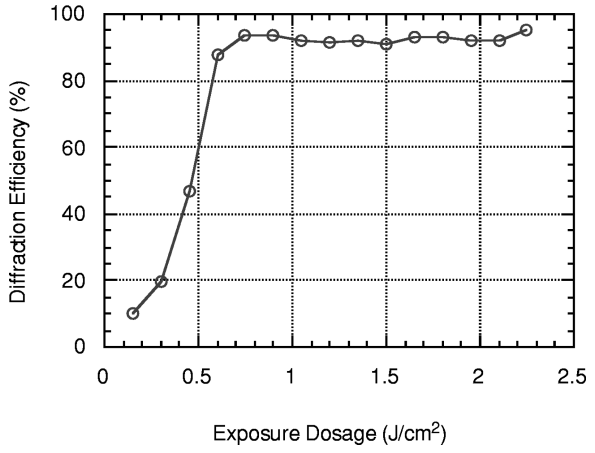

Fig. 4 Relation between diffraction efficiency and exposure dosage.

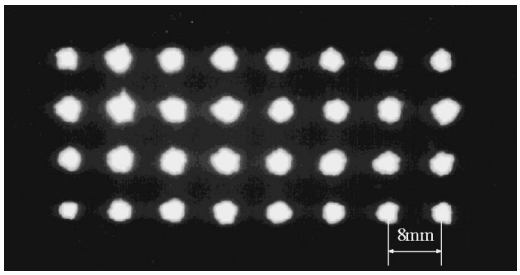

Fig. 5 CCD image of 5-bit delay fanout lines (4×8) with a fanout intensity fluctuation within 15%.

cies. It is plausible to fabricate the reported device with only two recording processes by tuning the intensity distribution of the recording beams.

4 Device Performance

A 1×4 broadband single-mode fiber beamsplitter with collimators at its output ends is packaged with the fabricated holographic input and output couplers on the substrate. The four output beams from the fiber beamsplitter are coupled into the substrate by the input couplers on the substrate. Figure 5 shows the image of 5-bit delay fanout lines (4×8) working in a transverse electric (TE) mode at 850 nm with a fanout intensity fluctuation within ±10%, as indicated in Fig. 6, which shows the relative intensities of the 32 fanouts. The packaging density of the device is 2.5 fanouts/cm^2. From the measured coupling efficiency, the system insertion loss is determined to be 18 dB, including an 8-dB insertion loss in the 1×4 fiber beamsplitter, a 9-dB fanout loss in the substrate guided wave, and 1 dB of propagation and other losses. The same results can be achieved with signals in a transverse magnetic (TM) mode.

The delay interval can be measured by employing a Ti:sapphire femtosecond laser system.[21] Figure 7 gives the schematic for measuring the fanout delay intervals. Two successive delay pulses from the TTD unit are combined with a focusing lens and coupled into a multimode fiber. In this way we are guaranteed that the two beams experience equal extra delays after being combined. The output of the fiber is fed into an ultrafast metal-semiconductor-metal

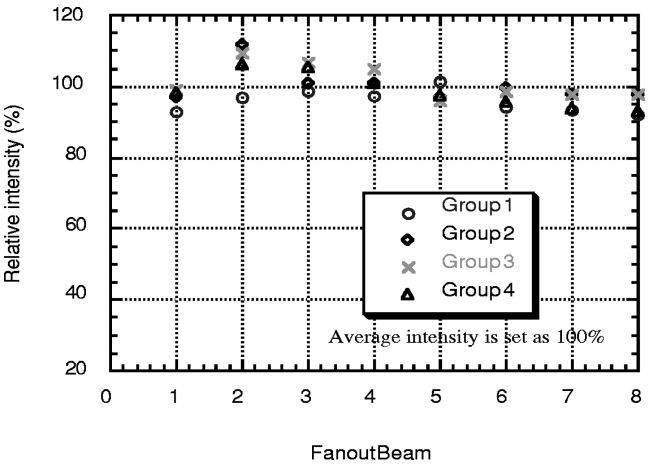

Fig. 6 Relative beam intensities of 32 fanouts from the TTD unit.

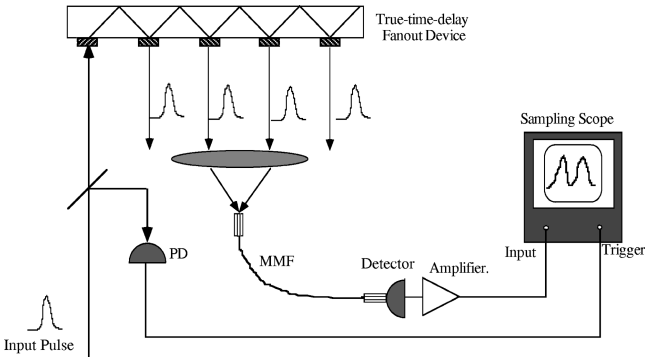

Fig. 7 Experimental setup for measuring the minimum delay interval.

(MSM) photodetector, which has a rise time of ≈7 ps. The output of the electrical response from the MSM detector is amplified through a 20-GHz 18-dB amplifier and later is connected to a sampling scope. The sampling scope is synchronously triggered by a reference pulse string from a monitoring photodiode output. As shown in Fig. 8, the delay between two successive fanouts is 50 ps.

The frequency range of the signal that can be carried by the device is limited by the dispersion among different wavelengths. The dispersion of the device is mainly due to two factors. One is the dispersion caused by hologram grating couplers. Since the diffraction angles of different incident wavelengths are different, the propagation lengths of different wavelengths after n reflections are different. Therefore, there is a group time delay between different wavelengths. The second factor is material dispersion caused by different phase velocities of different wavelengths. The contributions of these two factors to dispersion can be compensating.

The phase delay at the total-reflection surface is negligible because for different wavelengths the delays are almost the same. Based on these considerations, we can cal-

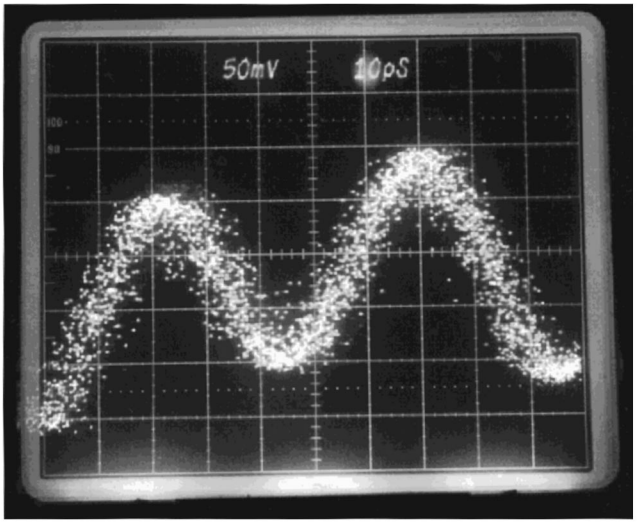

Fig. 8 Two pulses coming from successive fanouts with 50-ps delay between them.

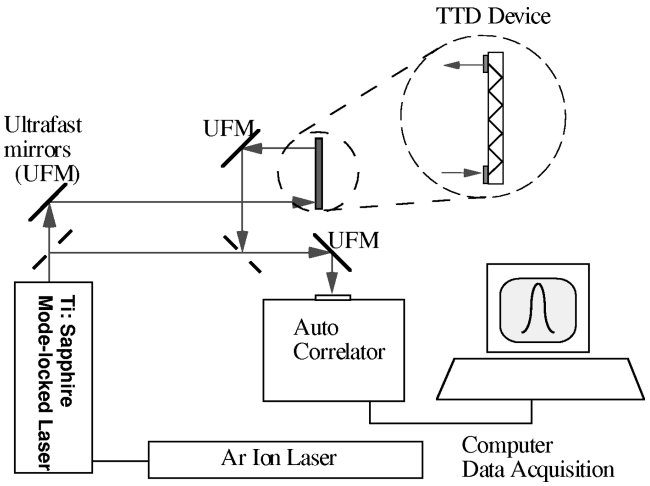

Fig. 9 Schematic for measuring the device bandwidth.

culate the dispersion as follows. The group delay τ is given by

$$\tau = \frac{2hmn_1}{\cos\theta_1 \cdot c} - \frac{2hmn_2}{\cos\theta_2 \cdot c} = \frac{2hm}{c}\left(\frac{n_1}{\cos\theta_1} - \frac{n_2}{\cos\theta_2}\right), \qquad (4)$$

where h is the height of the substrate, m is the number of zig-zag bounces, c is the velocity of light in free space, and θ is the bounding angle in the substrate. The period of a signal to be carried without error must be larger than this group delay. Therefore, the bandwidth is limited. The calculated bandwidth is about 2.0 THz.

The bandwidth of the TTD delay unit can be evaluated by measuring the femtosecond-laser-pulse widths before and after the device.[20] For this purpose, a femtosecond laser pulse is sent through the device. The pulse width of the later fanout beam having the longest propagation distance is measured and then compared with that of the incoming pulse. Fourier transformations are performed on both pulses to deduce the bandwidth of the device.

The experimental setup is shown in Fig. 9. An argon ion laser (INNOVA-90-PLUS) is used to pump a Ti:sapphire mode-locked laser (Clark-MXR model NJA-4), which provides pulses around 150 fs at the vicinity of 850 nm every 10 ns. An autocorrelator (Clark-MXR model AC-150) is employed to measure the pulse widths before and after entering the TTD device. To minimize any pulse broadening effect caused by the mirrors, two ultrafast mirrors (Newport 10B20UF.25) working at wavelengths ranging from 700 to 930 nm are used. The autocorrelator is driven by a computer-interfaced driver module (Clark-MXR ODL-1E) for calibration and data acquisition. Figure 10(a) illustrates the autocorrelation traces for the input (reference) and output (dispersed) pulses. The Fourier transform of the two pulses in the frequency domain yields bandwidth information about the device as shown in Fig. 10(b). The 3-dB bandwidth of the device is experimentally confirmed to be 2.4 THz, which is well matched with the theoretical prediction.

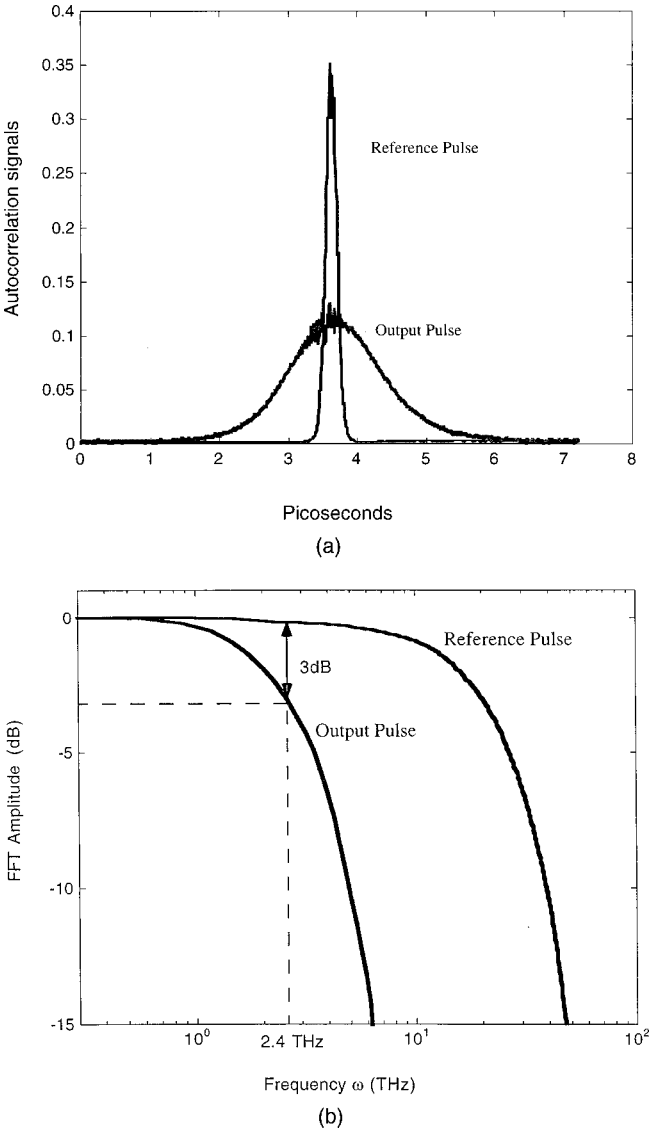

Fig. 10 (a) Pulse width measured before and after the TTD unit; (b) FFT power spectrum for the input and output pulses.

5 Conclusion

A 5-bit true-time-delay-line device having a packing density of 2.5 lines/cm^2 with a minimum delay step of 50 ps has been designed, fabricated, and demonstrated. The device is based on a fiber beamsplitter in conjunction with substrate guided wave propagation. The combined collinear fanouts are realized using slanted photopolymer volume phase grating arrays. The 5-bit delay lines are fabricated on 3-mm-thick quartz substrates with a substrate bouncing angle of 53.5 deg. The problem of power fluctuation among the outputs due to the cascading fanout effect has been experimentally investigated and solved. Power fluctuation has been controlled to within $\pm 10\%$ among 32 fanouts. A delay step of 50 ps with a 3-dB bandwidth of 2.4 THz is experimentally confirmed. The true-time delay device presented herein has the potential to be integrated with photodetector arrays to provide a planarized structure on a single substrate together with surface-normal fan-in and fan-out.

Acknowledgments

This research is sponsored by the Office of Naval Research, the DARPA Center for Optoelectronics Science and Technology, and the ATP program of the State of Texas. The authors would like to thank Dr. Yoon-Soo Park for his encouragement and support in this project.

References

1. A. A. Oliner and G. H. Knittel, *Phased Array Antennas*, Artech House, Dedham, MA (1972).
2. E. N. Toughlian and H. Zmuda, ''A photonic variable RF delay line for phased array antennas,'' *IEEE J. Lightwave Technol.* **8**(12), 1824–1828 (1990).
3. R. J. Mailloux, *Phased Array Antenna Handbook*, Artech House, Boston (1993).
4. H. Zmuda and E. N. Toughlian, *Photonic Aspects of Modern Radar*, Artech House, Boston (1994).
5. W. Ng, A. A. Walston, G. L. Tangonan, J. J. Lee, I. L. Newberg, and N. Bernstein, ''The first demonstration of an optically steered microwave phased array antenna using true-time delay,'' *IEEE J. Lightwave Technol.* **9**(9), 1124–1131 (1991).
6. A. Goutzoulis and K. Davies, ''All-optical hardware-compressive wavelength-multiplexed fiber optic architecture for true-time delay steering of 2-D phased array antennas,'' *Proc. SPIE* **1703**, 604–614 (1992).
7. L. J. Lembo, T. Holcomb, M. Mickham, P. Wisseman, and J. C. Brock, ''Low-loss fiber optic time-delay element for phased-array antennas,'' *Proc. SPIE* **2155**, 13–23 (1994).
8. W. Ng, D. Yap, A. Narayanan, R. Hayes, and A. Wilston, ''A detector-switched GaAs monolithic time-delay network for microwave phased arrays at L and X band,'' in *Topical Meeting on Integrated Photonics Research, IWA4*, OSA, pp. 418–421 (1993).
9. C. T. Sullivan, S. D. Mukherjee, M. K. Hibbs-Brenner, and A. Gopinath, ''Switched time delay elements based on AlGaAs/GaAs optical waveguide technology at 1.32 μm for optically controlled phased array antennas,'' *Proc. SPIE* **1703**, 264–271 (1992).
10. E. J. Murphy, T. F. Adda, W. J. Minford, R. W. Irvin, E. I. Ackerman, and S. B. Adams, ''Guided-wave optical time delay network,'' *IEEE Photonics Technol. Lett.* **8**(4), 545–547 (1996).
11. L. H. Gesell, R. E. Feinleib, J. L. Lafuse, and T. M. Turpin, ''Acousto-optic control of time delays for array beam steering,'' *Proc. SPIE* **2155**, 194–204 (1994).
12. D. T. K. Tong and M. C. Wu, ''A novel multiwavelength optically controlled phased array antenna with a programmable dispersion matrix,'' *IEEE Photonics Technol. Lett.* **8**(6), 812–814 (1996).
13. R. T. Chen and R. Lee, ''Holographic optical elements (HOEs) for true-time delays aimed at phased array antenna applications,'' *SPIE Tech. Digest* **2689**, 176–187 (1996).
14. R. Li and R. Chen, ''3-bit substrate-guided-mode optical true-time-delay lines operating at 25 GHz,'' *IEEE Photonics Technol. Lett.* **9**(1), 100–102 (1997).
15. M. R. Wang, G. J. Sonek, R. T. Chen, and T. Jannson, ''Large fanout optical interconnects using thick holographic gratings and substrate wave propagation,'' *Appl. Opt.* **31**(2), 236–249 (1992).
16. R. T. Chen, S. Tang, M. Li, D. Gerald, and S. Natarajan, ''1-to-12 surface normal three dimensional optical interconnects,'' *Appl. Phys. Lett.* **63**(14), 1883–1885 (1993).
17. J.-H. Yeh and R. K. Kostuk, ''Substrate-mode holograms used in optical interconnects: design issues,'' *Appl. Opt.* **34**(17), 3152–3164 (1995).
18. W. J. Gambogi, A. M. Weber, and T. J. Trout, ''Advances and application of DuPont holographic photopolymers,'' *Proc. SPIE* **2043**, 2–13 (1993).
19. U. Rhee, J. J. Caulfield, C. S. Vikram, and J. Shamir, ''Dynamics of hologram recording in DuPont photopolymer,'' *Appl. Opt.* **34**(5), 846–852 (1995).
20. W. J. Gambogi, W. A. Gerstadt, S. R. Mackara, and A. M. Weber, ''Holographic transmission elements using improved photopolymer films,'' *Proc. SPIE* **1555**, 256–267 (1991).
21. R. Li, Z. Fu, and R. Chen, ''High density broadband true-time-delay unit on a single substrate,'' *Proc. SPIE* **3006**, 256–263 (1997).

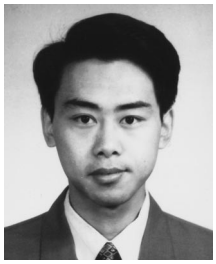

Zhenhai Fu received his BS degree in 1993 and MS degree in 1996, both in optical instruments, from Zhejiang University, Hangzhou, China, and Tsinghua University, Beijing, China, respectively. He is currently a PhD candidate in the Department of Electrical and Computer Engineering at the University of Texas at Austin. The main fields of his research are optoelectronics devices, optical communication, phased array antennas, and microwave devices and systems. He is a student member of SPIE and IEEE/LEOS.

Ray T. Chen is currently with the Microelectronics Research Center of the Department of Electrical and Computer Engineering at the University of Texas, Austin. Dr. Chen's research group has been working on over 40 awarded research programs sponsored by many subdivisions of DOD, NSF, DOE, NASA, the State of Texas, and other private industries such as Cray Research, GE, Honeywell, 3M, Boeing, Physical Optics Corporation, MCC, and Novex Corp. The research topics cover guided wave and free-space optical interconnects, polymer-based integrated optics, polymer waveguide amplifier, GRIN polymer waveguide lenses, active optical backplanes, traveling wave electrooptic polymer waveguide modulators, optical control of phased array antenna, GaAs all-optical cross-bar switch, holographic lithography and holographic optical elements. Dr. Chen, the group leader and an associate professor in the ECE Department, has served as the chairman and program committee member for over 25 domestic and international conferences organized by SPIE (The International Society of Optical Engineering), OSA, IEEE, and PSC. He is also an invited lecturer for the short course on optical interconnects for the international technical meetings organized by SPIE. The optical interconnects research group at UT Austin has published over 200 research papers including 35 invited papers. Chen has served as a consultant for various federal government agencies and private companies and delivered numerous invited talks in the professional societies. Dr. Chen is a member of IEEE, LEOS, SPIE, OSA, and PSC and holder of the Temple Foundation Endowed Faculty Fellowship No. 4. Currently there are 14 PhD students and four postdoctoral students working on optical interconnects-related projects.